A Decade of Ground–Air Temperature Tracking at Emigrant Pass Observatory, Utah

MARSHALL G. BARTLETT

Department of Biochemistry and Physical Sciences, Brigham Young University—Hawaii, Laie, Hawaii

DAVID S. CHAPMAN

Department of Geology and Geophysics, University of Utah, Salt Lake City, Utah

ROBERT N. HARRIS

College of Oceanic and Atmospheric Sciences, Oregon State University, Corvallis, Oregon

(Manuscript received 30 June 2005, in final form 14 November 2005)

ABSTRACT

Observations of air and ground temperatures collected between 1993 and 2004 from Emigrant Pass Geothermal Climate Observatory in northwestern Utah are analyzed to understand the relationship between these two quantities. The influence of surface air temperature (SAT), incident solar radiation, and snow cover on surface ground temperature (SGT) variations are explored. SAT variations explain 94% of the variance in SGT. Incident solar radiation is the primary variable governing the remaining variance misfit and is significantly more important during summer months than winter months. A linear relationship between the ground–air temperature difference ($\Delta T_{\text{sgt-sat}}$) and solar radiation exists with a trend of 1.21 K/(100 W m^{-2}); solar radiation accounts for 1.3% of the variance in SGT. The effects of incident solar radiation also account for the 2.47-K average offset in $\Delta T_{\text{sgt-sat}}$. During the winter, snow cover plays a role in governing SGT variability, but exerts only a minor influence on the annual tracking of ground and air temperatures at the site, accounting for 0.5% of the variance in SGT. These observations of the tracking of SGT and SAT confirm that borehole temperature changes mimic changes in SAT at frequencies appropriate for climatic reconstructions.

1. Introduction

The observed 0.7 K of warming in the meteorological record over the past 150 yr serves as an important piece of evidence that the climate system is changing (Jones and Moberg 2003; Houghton et al. 2001). The meteorological record, however, is too short to reliably determine how much of the observed warming is directly related to anthropogenic activities and how much is a natural variation in the earth's background climate (Karl et al. 1989; Houghton et al. 2001). Recently, geothermal studies have utilized temperature variations in the upper few hundred meters of the earth's crust to provide a climatic reference from which to understand the warming in the meteorological record (Beltrami 2002; Harris and Chapman 2001; Huang et al. 2000).

Borehole temperature–depth profiles contain climatic information related to surface ground temperature (SGT) history. Ground surface warming or cooling imparts a temperature perturbation to the subsurface that propagates downward and is superimposed on the background thermal field. Excursions in average surface temperature beginning 10, 100, and 1000 yr ago produce temperature anomalies centered at depths of 25, 80, and 250 m, respectively. These subsurface temperature profiles are important indicators of ground surface climate change. However, they also contain information complementary to surface air temperature (SAT) records (Smerdon et al. 2004; Harris and Chapman 1998, 2001). Meaningful comparisons of SGT and SAT depend on consistent tracking between these two sources of climate information. Quantifying the relationship between ground and air temperatures and understanding the processes that facilitate or hinder track-

Corresponding author address: Dr. Marshall G. Bartlett, Department of Biochemistry and Physical Sciences, Brigham Young University—Hawaii, 55-220 Kulanui Street, Laie, HI 96762.
E-mail: bartletm@byuh.edu

ing between the two are important steps in validating the use of temperature–depth profiles in climate studies and comparisons to proxy-based reconstructions.

On long time scales, the ground–air interface is in energy equilibrium, and the corresponding temperatures measured in each medium reflect this energy balance. However, time-varying thermal properties and complicated energy exchange mechanisms across the ground–air interface make a detailed accounting at any moment in time a daunting task (Delworth and Knutson 2000). Surface characterization and land surface process models capture the general movements of heat and mass at the ground–air interface, but do not predict transient temperature changes with the subdegree accuracy required to understand ground–air tracking (Soet et al. 2000). In this study, we measure temperatures across the ground–air interface to understand the energy balance at this boundary. We examine the temperature difference ($\Delta T_{\text{sgt-sat}}$) between the ground surface and the air column at 2 m and interpret these observations in terms of observed changes in the surface boundary condition from sources including meteorological variations in solar insolation and the presence or absence of snow cover.

Many studies have investigated the planetary boundary layer, and have described the mechanisms of heat transport at the ground–air interface. The early work of Geiger (1965) set the stage for rigorous scientific work, and today there are numerous groups developing computer models to simulate the complex physics at the interface (e.g., Soet et al. 2000; Irannejad and Shao 1998). Observational studies of surface temperature have tended to be in the agricultural area and have focused on water and gas transport across the interface (Hu and Islam 1995; Tan and Layne 1993; Parton 1984). Detailed tracking studies of air and ground temperatures have been conducted by several research groups in a variety of locales (Baker and Ruschy 1993; Beltrami 2001; Schmidt et al. 2001; Putnam and Chapman 1996). More recently, computer simulations of ground–air tracking have been undertaken (Gonzalez-Rouco et al. 2003).

This study examines observational data from Emigrant Pass Observatory (EPO) in northwestern Utah to quantify the processes that influence the relationship between SGT and SAT. Repeat borehole temperature logs at the site reveal that transient changes in the upper part of the temperature–depth profile can be attributed to changes in the surface temperature through time using a simple 1D model of heat conduction (Chapman and Harris 1993). Inferred surface temperature changes are similar to those observed at the nearest meteorological station 40 km to the northeast (Chisholm and Chapman 1992). To better understand the surficial processes affecting the relationship between ground and air temperatures in greater detail, meteorological instrumentation and ground temperature sensors were installed in November 1993. The first annual cycle of these data was reported by Putnam and Chapman (1996). The observatory has operated continuously since the fall of 1993. In this study, we analyze the data through July of 2004, more than 10 yr of observations.

2. Emigrant Pass Observatory

Emigrant Pass Observatory (Fig. 1) is located on the eastern flank of the Grouse Creek Mountains in the Basin and Range province in the northwest region of the state of Utah (41°30′N, 113°42′W; elevation 1750 m). Topography within 300 m of the site is roughly planar and gently sloping downward to the northeast. The vegetation consists of juniper and pinyon pines, which are spaced about 5 m apart and reach a maximum height of 3 m.

The observatory was installed at the site of borehole Grouse Creek 1 (GC-1), drilled in 1978 to a depth of 150 m as part of a regional heat flow study (Chapman et al. 1978). The borehole is sited in an exposed granite pluton where thermal conductivity variations are small and hydrologic flow is negligible (Chisholm and Chapman 1992).

Instrumentation at EPO (Table 1) consists of a solar powered Campbell Scientific CR-10 data logger controlling a suite of meteorological instruments plus two shallow thermistor strings designed to measure temperature in the granite outcrop and nearby regolith. The meteorological instruments include air temperature, solar radiation, precipitation, snow depth, wind speed, and wind direction. A data logger interrogates the sensors every 60 s and stores 30-min averages. A comprehensive review of the sensors, including the installation, setup, and calibration, is given in Putnam and Chapman (1996).

Battery failures, occasional sensor failures, and program errors have contributed to some data gaps in the record from EPO. Approximately 15% of the data is missing from the air temperature record (Table 1), and as much as 40% of the data from some of the ground temperature sensors is missing. The largest single data gap covers nearly an entire annual cycle (October 2001–September 2002) and was caused by a data storage module failure. The next longest gap (nearly 3 months long) was due to a battery failure in the winter of 1996–97. Smaller data gaps result from unstable voltage inputs in the data logger and/or intermittent sensor

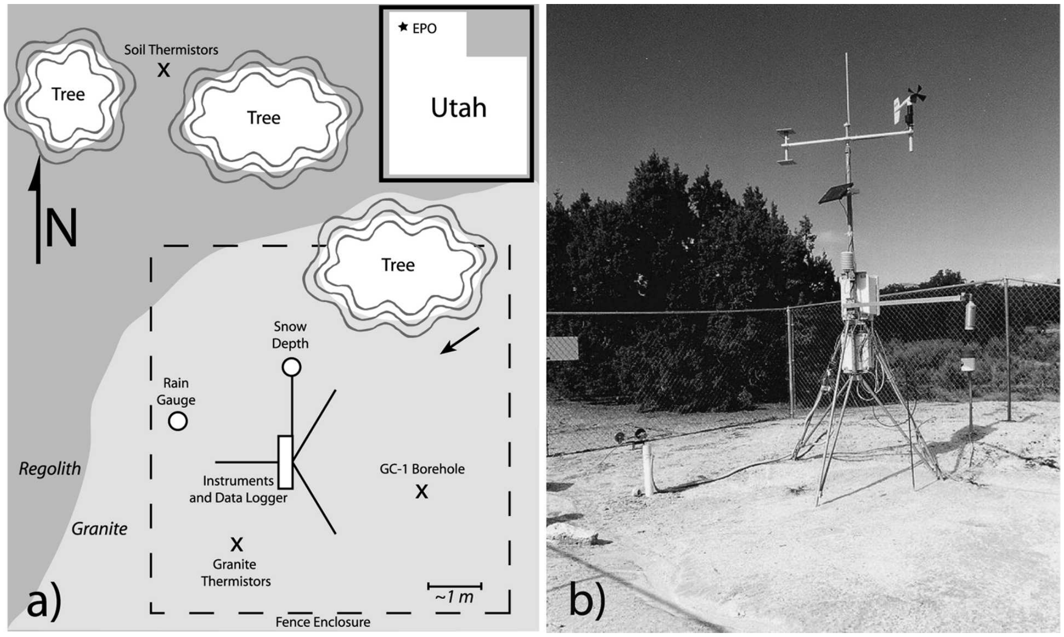

FIG. 1. (a) Location and schematic map of EPO and (b) image of the site. The weather station is located on a granite outcrop and immediately adjacent to borehole GC-1. The majority of these instruments are located on a tripod mast along with the data logger. Sensors for ground temperatures to 1.0-m depth are located in the granite and in the nearby regolith. The arrow in (a) illustrates the approximate position and direction from which photo (b) was taken.

and instrument failures. In October 2004, EPO was upgraded. Five new ground thermistor strings were installed at the site along with updated meteorological equipment. Data from the station is now collected via cellular uplink on a daily basis. Since the upgrades, the data return rate from EPO has been 100%.

The simple geology, flat topography, and arid climate at EPO provide a relatively uncomplicated site to measure heat transfer at the earth's surface and to test temperature tracking at the ground–air interface. For other more complicated environments with significant moisture, advective water flow, and/or changing vegetation, the ground–air temperature tracking is undoubtedly more complex.

3. Direct ground and air temperature comparisons at EPO

Previous work comparing ground and air temperatures at EPO indicates that heat transfer in the ground

TABLE 1. Instrumental summary of EPO.

Measured parameter	Precision	Installation	Completeness %*
Air temperature	0.05 K	2 m above granite	85
Air temperature**	0.05 K	0.1 m above regolith	33
Granite temperature	0.01 K	0.025, 0.1, 0.2, 0.5, 1.0 m	33, 70, 62, 62, 58
Regolith temperature	0.01 K	0.025, 0.1, 0.2, 0.5, 1.0 m	39, 41, 21, 41, 43
Solar radiation	0.1 W m^{-2}	Incident and reflected	85
Rainfall	0.1 mm	1-m mast height	85
Snow depth	1.0 mm	Sonar "pinger"	46
Wind speed	0.04 m s^{-1}	3-m mast height	85
Wind direction	5.0°	3-m mast height	85
Humidity	1%–3%	2 m	85
Soil moisture**	1%–5%	0.1, 0.5 m	11

* Completeness is (%) of 60-s samples over the period, 1993–2004.
** Installed in March 1997.

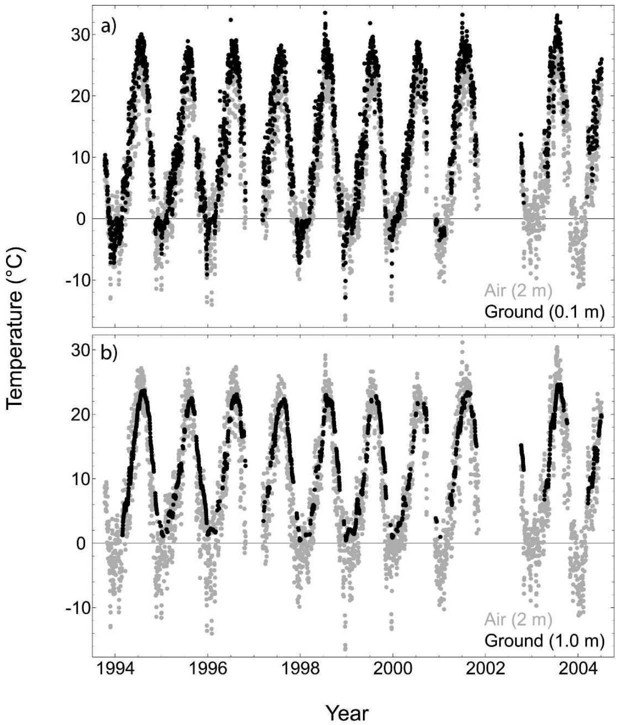

FIG. 2. Comparison of air and ground temperature at EPO during 1993–2004. (a) Ground temperatures at 0.1 m retain much of the same frequency information as is contained in the air temperature observations. Excess ground temperature warming is apparent during the summer months as is the influence of snow cover during the winter. (b) At a depth of 1.0 m, much of the high-frequency information is no longer present in the ground temperature record and there is a significant phase shift and attenuation of the record compared to the air.

is primarily through 1D diffusion (Putnam and Chapman 1996; Chapman and Harris 1993; Chisholm and Chapman 1992). Direct comparisons between measured temperature–time series demonstrate the simple heat flow regime. Figure 2 shows the mean daily air temperature at 2-m height compared with the mean daily granite temperature at 0.1- and 1.0-m depths below the surface over the period 1993–2004. Daily mean values are computed from the 30-min observations. Gaps represent missing data or days with an incomplete record (fewer than 48 observations per day). Daily mean surface air temperature at EPO varies by 40 K over the annual cycle, from 30°C in midsummer to −10°C in midwinter. Extreme daily air and ground temperatures extend that range by an additional 14 K in some years. Both air and ground temperatures have a dominant annual period with important higher-frequency components.

The subsurface temperatures at both 0.1 m (Fig. 2a) and 1.0 m (Fig. 2b) are in general agreement with the air temperature. Quantitatively, air and ground temperatures are strongly correlated, with correlation coefficients of 0.97 and 0.87 for the 0.1- and 1.0-m observations, respectively. Air temperatures explain 90% of the variance observed in the daily mean ground temperatures at 0.1 m. However, the point-to-point temperature difference between the ground at 1-m depth and the air at 2-m height can easily be as much as +10 and −10 K on the same day. This difference is a consequence of the phase lag and attenuation associated with thermal diffusion into the ground rather than meteorological phenomena at the ground–air interface. To quantify the tracking of air and ground temperatures more precisely, we must account for the effects of heat diffusion in the subsurface observations.

4. Ground surface temperatures at EPO

If we could measure the surface ground temperature directly, the effects of phase lag and attenuation associated with heat diffusion would be eliminated. Direct measurement of the ground "skin" temperature, however, is difficult because any measuring device on the surface disrupts the thermal properties of the surface and therefore the measurement itself. Although direct radiometric measurements of skin temperature avoid the thermal disturbance problem, they can only achieve a precision of about 0.5 K and require a very high sampling interval (<60 s) to capture the enormous variability faithfully. Another drawback to radiometric measurements of surface temperature is that they measure the temperature at the top of the snowpack, or flooded surface, rather than the temperature of the actual ground surface. Instead, we estimate ground surface temperature by solving the inverse heat conduction problem using measured temperature–time series at a fixed depth within the ground. This method of estimating surface temperature from subsurface temperature measurements provides an accurate, albeit time-averaged, value for the surface temperature and effectively corrects for the phase lag and attenuation associated with observations at finite depth.

The propagation of temperature in the ground is described by the 1D heat diffusion equation,

$$\frac{\partial}{\partial t} T(z, t) = \alpha_{\mathrm{eff}} \frac{\partial^2}{\partial z^2} T(z, t), \tag{1}$$

where T is temperature, t is time, z is depth, and α_{eff} is the apparent diffusivity (Carslaw and Jaeger 1959). When temperatures from multiple depths are known, the only unknown parameter in Eq. (1) is α_{eff}. Since surface temperature changes can be expressed as a se-

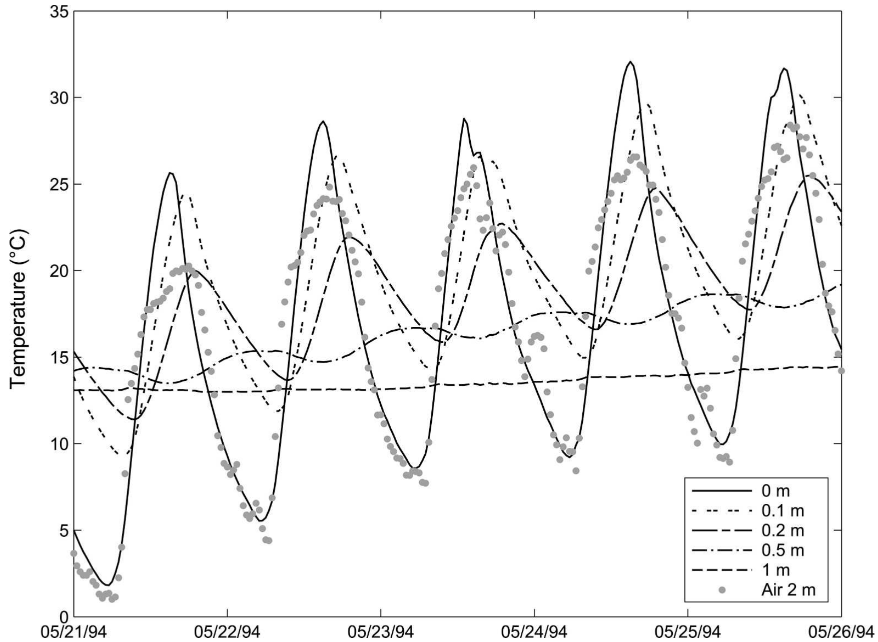

FIG. 3. An example of SGT reconstruction at EPO from temperature observations at depth. The surface temperature–time series is reconstructed using information contained in the observations at multiple depths within the ground layer. The reconstructed surface temperature is warmer than the observed air temperature during the daylight hours because of incident solar radiation, but follows the air temperature closely at night.

ries of step changes, the error function solution to Eq. (1) given by Carslaw and Jaeger (1959),

$$T(z,t) = \sum_{n=t_0}^{t} (T_n - T_{n-1}) \times \mathrm{erfc}\left[\frac{z_{\mathrm{obs}} - z}{\sqrt{4\alpha_{\mathrm{eff}}(t_n - t_0)}}\right] \tag{2}$$

is applicable, where z_{obs} is the depth of observation and erfc is the complementary error function. We can estimate in situ values of α_{eff} by propagating temperature observations from multiple depths downward and adjusting α_{eff} to minimize the misfit between the calculated time series and the observations. Putnam and Chapman (1996) report a mean diffusivity value of 0.88×10^{-6} m^2 s^{-1} for the upper meter of granite at EPO, based on observations between 1993 and 1994. We extend this calculation over the period 1993–2004 and find that daily mean α_{eff} at EPO in the granite layer (0.1–1.0 m) has a range of $0.78–0.96 \times 10^{-6}$ m^2 s^{-1}, a mean value of 0.88×10^{-6} m^2 s^{-1}, and a standard deviation of 0.05×10^{-6} m^2 s^{-1}. The apparent diffusivity in the regolith layer (0.1–1.0 m) is considerably smaller with a mean value of 0.65×10^{-6} m^2 s^{-1} and a range of 0.42–0.83×10^{-6} m^2 s^{-1}.

Using this value of α_{eff} and observations of temperature from 0.1-m depth within the granite, we solve Eq. (1) for the temperature at the ground surface ($z = 0$). The observations at 0.1 m are chosen because this is the most reliable ground thermistor (Table 1) and because this depth preserves much of the high-frequency surface variation. We employ a regularized inversion method to solve Eq. (2) for the temperature–time series at the surface ($z = 0$), given the temperature–time observations at 0.1-m depth. The calculated temperature–time series, $T(z, t)$, does not exactly reproduce the frequency information of the true temperature time series because with increasing depth information, it is lost through diffusion. The calculated temperature–time series at $z = 0$ has greater amplitude than that at $z = 0.1$ m, but does not contain frequencies higher than those in the observations at 0.1 m. Application of this technique to the reconstruction of observed time series (reconstructing the observations at 0.1 m from those at 0.2 m, for example) produces results with rms errors less than 0.05 K, a value roughly equivalent to the precision of the thermistors.

Figure 3 shows 5 days of our calculated surface temperature in May of 1994. The surface temperature leads the temperature oscillations at successive depths, and the diurnal variation is much greater at the surface than it is at 0.1 m. These features are attributable to the phase lag and attenuation associated with thermal diffusion. Surface ground temperature almost matches the surface air temperature during the night, but can be significantly warmer (>5 K) during the daylight hours. As discussed below, this warming during the daytime is principally due to the influence of incident solar radiation.

5. Ground–air temperature tracking at EPO

Estimates of the surface ground temperature ($z = 0$) at EPO allow direct comparisons between ground and air temperatures. Figure 4 illustrates the difference ($\Delta T_{\text{sgt-sat}}$) between calculated SGT and observed SAT for the period 1993–2004. When the effects of diffusion are restored to the SGT inferred from the ground temperature observations at 0.1 m, the percentage of variance in the SGT explained by the SAT observations increases from 90% to 94%. These numbers indicate the importance of accounting for the effects of diffusion.

However, even with the effects of diffusion, a seasonal offset between ground and air temperatures is apparent in all years of observation. This offset is largest during the summer (averaging about 5 K) and falls to nearly 0 K during the winter. The 1993–2004 mean $\Delta T_{\text{sgt-sat}}$ is 2.47 K. It varies from −10 to +14 K when averaged over a diurnal cycle. This offset is consistent with excess heating of the ground due to incident solar radiation during the summer months (Putnam and Chapman 1996). The sensitivity of $\Delta T_{\text{sgt-sat}}$ at EPO to incident solar radiation is largely attributable to the

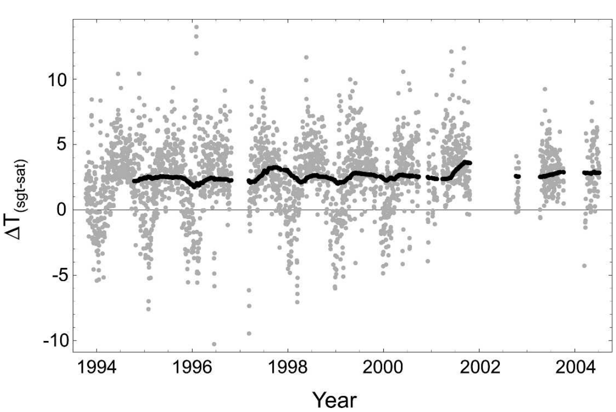

FIG. 4. Difference between SGT and SAT observations at EPO during 1993–2004. The gray dots indicate the daily mean temperature difference; the black dots are a backward looking 365-day average of the daily observations. Where missing data are encountered, the mean values for all observations with the same Julian day are used as to fill in for the backward looking filter. The persistent 2.47-K offset is ground warming resulting from incident solar radiation during the summer months. The filtered observations indicate that interannual variability is ~1 K.

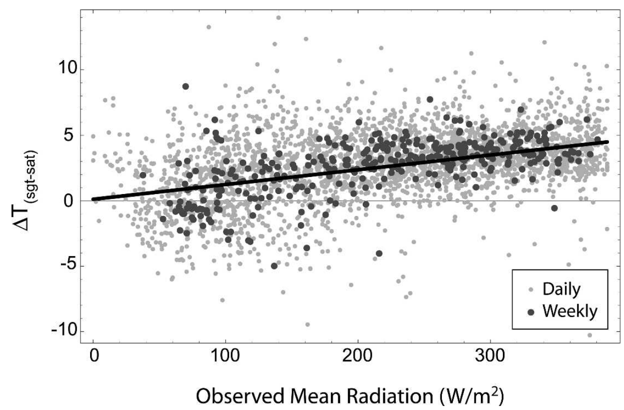

FIG. 5. Relationship of ground–air temperature difference and incident solar radiation at EPO during 1993–2004. The gray points represent the daily values of the ground–air temperature difference and the observed solar radiation; the larger black dots are weekly mean values. Greater coherence in the relationship is observed above 180 W m^{-2}. The solid line has a slope of 1.21 K/(100 W m^{-2}) of radiation.

specific surface conditions at the site and may not be a general feature of the ground–air tracking at other locations. In particular, the lack of vegetation at the surface and the low porosity (water content) of the granite at EPO minimize the latent heat effects of water at the ground–air interface, increasing the temperature signature associated with radiant heating. This characteristic makes EPO a particularly interesting site for the study of solar influences on ground–air temperature tracking.

To understand the magnitude of incident solar radiation on $\Delta T_{\text{sgt-sat}}$, we plot daily and weekly values of $\Delta T_{\text{sgt-sat}}$ against observed radiation (Fig. 5). The high degree of interday variability, particularly for observed radiation values below 180 W m^{-2}, reflects the variability of meteorological conditions at the site. Nevertheless, a generally linear correlation between $\Delta T_{\text{sgt-sat}}$ and observed incident solar radiation exists. The correlation improves when mean weekly values of solar radiation and $\Delta T_{\text{sgt-sat}}$ are considered. This improvement is consistent with the notion that the variability is, to a large degree, attributable to daily weather phenomena. Fitting a linear trend to the data in Fig. 5 suggests that for each 100 W m^{-2} of incident radiation, the ground becomes, on average, 1.21 K warmer than the air at the site.

Table 2 summarizes the radiation observations at EPO, the magnitude of the correction calculated for each calendar year, and the percentage of daily observations available from each year. Where daily observed values of incident solar radiation are unavailable, mean values for the same Julian date from other years of observation are used as fill-ins in calculating the mean,

TABLE 2. Annual summary of radiation observations at EPO.

Year	Mean W m^{-2}	Standard deviation W m^{-2}	Annual radiation correction K	Data coverage %
1994	203.0	101.3	2.46	95.6
1995	193.7	96.1	2.34	95.3
1996	202.4	99.2	2.45	78.6
1997	196.6	96.0	2.38	77.5
1998	191.1	98.1	2.31	100.0
1999	190.5	103.1	2.31	100.0
2000	199.3	97.3	2.41	78.1
2001	207.1	99.9	2.51	85.5
2002	200.1	87.4	2.42	23.0
2003	204.5	100.8	2.47	100.0

standard deviation, and correction in Table 2. No long-term trend in annual incident solar radiation is observed, though interannual variations of as much as 15 W m^{-2} exist.

The linear trend between incident solar radiation and $\Delta T_{\text{sgt-sat}}$ suggests that we can adjust $\Delta T_{\text{sgt-sat}}$ for the influence of radiation. This adjustment is illustrated in Fig. 6. Comparing Fig. 6 to Fig. 4 illustrates several important features of the ground–air temperature tracking at EPO. First, as expected, adjusting for the radiation trend effectively removes both the 2.47-K annual offset and most of the seasonal variation present in Fig. 4, indicated by the gray dots. Second, adjusting $\Delta T_{\text{sgt-sat}}$ for radiation also removes most of the interannual variability in $\Delta T_{\text{sgt-sat}}$, as indicated by the black line. This is particularly evident when one compares the annually filtered results in Figs. 4 and 6, which have standard deviations of 0.49 and 0.26 K, respectively. In terms of the variance in the data, including the influence of solar radiation explains an additional 1.3% of the variance in SGT. The efficacy of this adjustment in reducing the interannual variability suggests that much of the variability in $\Delta T_{\text{sgt-sat}}$ on decadal time scales is a result of changing incident solar radiation due to increased or decreased cloud cover. The geographic location of EPO within the zone of interannual jet stream variability means that annual cloud cover at the site is strongly tied to climatic oscillations in the Pacific Ocean. These oscillations lead to changes in the seasonal pattern of high and low pressure over western North America, which then have a large influence on the track that weather systems take over the continent (Peixoto and Oort 1992). It seems quite probable that as a result of the number of these weather systems that pass over EPO in a given year and the associated increase or decrease in cloud cover, $\Delta T_{\text{sgt-sat}}$ at the site is responding, in part, to regional climate variations. Finally, a comparison of Figs. 4 and 6 also indicates that despite correcting for radiation effects, interesting periods of variability in $\Delta T_{\text{sgt-sat}}$ still remain. This variability is connected to periods of snow cover at the site. Observed periods of snow at EPO are highlighted by the light gray bars in Fig. 6.

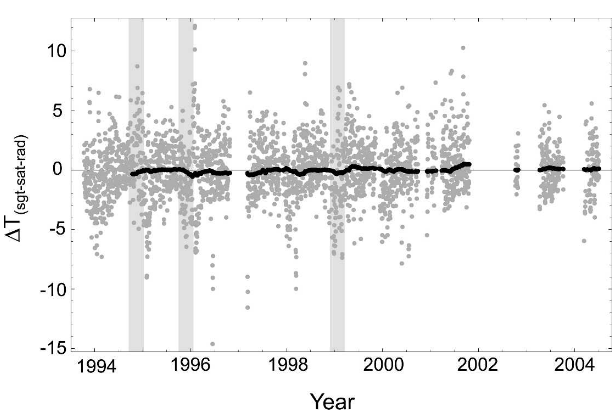

FIG. 6. Radiation-adjusted ground–air temperature difference at EPO during 1993–2004. As in Fig. 4, the gray dots represent the daily temperature difference while the black dots are a backward looking 365-day average. A simple linear adjustment for radiation not only removes the 2.47-K offset in the record but also removes the majority of the interannual variability observed in Fig. 4, suggesting that the interannual variability is a result of changes in annual cloud cover at the site. The light gray bars indicate winters with observed snow cover. Despite the radiation adjustment, these locations seem to have greater scatter in the ground–air temperature difference than other portions of the record. At least one other snow event has occurred at EPO during the 1997–98 winter season, but because of an instrumentation failure at the site, no snow depth observations were made.

Bartlett et al. (2004) developed a snow-ground thermal model using data from EPO to elucidate the impact of snow cover on ground–air temperature differences. Applying the snow-ground thermal model to the observations at EPO produces a daily "snow effect"—the difference between ground surface temperatures with snow cover and those predicted if snow had been absent. Just as a linear model of the impact of radiation on SGT could be used as an update, results of the snow-ground thermal model can also be used to effectively account for the impact of snow cover on $\Delta T_{\text{sgt-sat}}$.

For the three snow events observed at EPO (1994–95, 1995–96, and 1998–99), the snow-ground thermal model corrected values of $\Delta T_{\text{sgt-sat}}$ are illustrated in Fig. 7. Accounting for the influence of snow cover during the first two snow events leads to a significant seasonal decrease in the variability in $\Delta T_{\text{sgt-sat}}$. This calculation suggests that snow cover at EPO during the winter months does not bias the $\Delta T_{\text{sgt-sat}}$ offset so much as it adds increased variability to the day-to-day tracking of ground and air temperatures. Accounting for the pres-

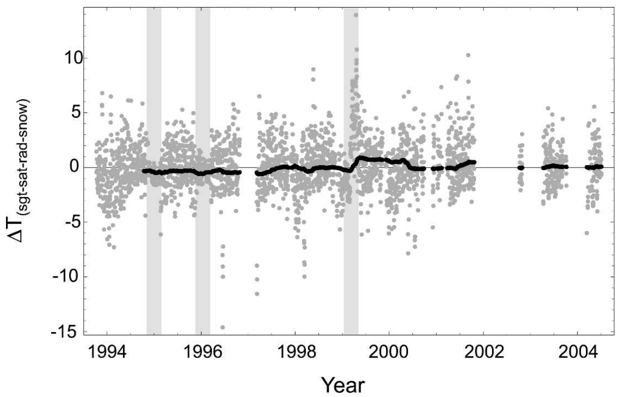

FIG. 7. Snow- and radiation-adjusted ground–air temperature difference at EPO during 1993–2004. The snow-ground thermal model of Bartlett et al. (2004) is used to account for the presence of snow cover on the ground. In two of the three observed snow events, the model adjustments significantly reduce the amount of scatter in the temperature difference. The model's adjustment for the 1998–99 snow event, however, leads to a large positive temperature difference anomaly.

ence of snow during the 1998–99 snow event, however, leads to an increase in $\Delta T_{sgt\text{-}sat}$. While the 1994–95 and 1995–96 snow events are fairly monoepisodic in nature with a definite single onset and duration, the 1998–99 event is fractured during the snow season (Fig. 8). Judging by the extremely shallow depths of the final two portions of the 1998–99 event, these observations are likely measurements of drifting snow captured in the small microtopographic depression beneath the snow sensor at EPO, and are not representative of conditions at the ground thermistor a few meters away (Fig. 1). Consequently, we interpret the increased variability during the second half of this event to be a result of the snow-ground thermal model being influenced by a local site condition, namely, the offset of approximately 3 m between the snow depth sonic ranger and the ground thermistors. Across all years at EPO, snow has a relatively weak influence on ground temperatures. Correcting for its influence explains only 0.5% of the remaining variance in SGT.

6. Discussion

A motivation behind this study is to better understand the relationship between air and ground temperatures. This understanding is important because while interpreting borehole temperature–depth profiles strictly in terms of climate change only gives variation in SGT, there is a great benefit to being able to tie these interpretations to SAT variations (Harris and Chapman 1998, 2001). The validity of this link lies in the nature of the relationship between ground and air temperatures.

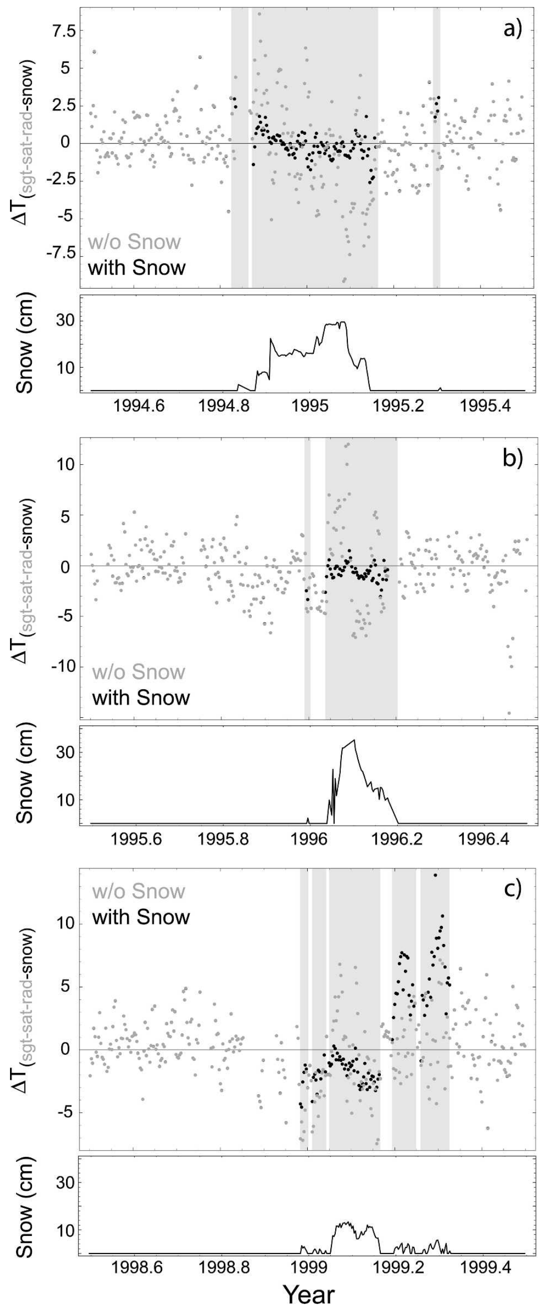

FIG. 8. Details of the three observed snow events at EPO and their impact on the ground–air temperature difference. The (a) 1994–95 and (b) 1995–96 snow events are relatively monoepisodic in nature. The snow-ground thermal model adjustment significantly reduces the scatter in the temperature difference in both cases. The (c) 1998–99 snow event is more fractured than the previous two. During the first half of this event, the model again reduces the scatter in the temperature difference. However, the two shallow snow depth periods in the spring lead to a significant amount of bias introduced by the snow adjustments. This bias is likely caused by small amounts of drift snow being present under the acoustic snow ranging instrument (and being used in the model) but not actually being present at the location of the ground thermistors.

Many borehole climate studies assume that $\Delta T_{\text{sgt-sat}}$ is unknown, but constant over long time scales, and that the transient temperature changes at the ground surface are equivalent to the transient changes measured on the meteorological mast. Our results here suggest that at EPO, this assumption is warranted over the past decade.

At EPO, transient temperature changes at the ground surface track changes in air temperature very well. Although the exact moment-to-moment mechanisms of heat transport are complicated, simple 1D conductive modeling produces an elegantly simple result when averaged over an annual cycle. While time-varying thermal diffusivity, latent heat associated with freeze–thaw cycles, and evaporation complicate the heat transfer, the net effect of these processes over the course of a decade of observations at the site is negligible.

To first order, the value of $\Delta T_{\text{sgt-sat}}$ at EPO is governed by the amount of solar radiation (1.21 K per 100 W m^{-2}). The ground surface at EPO receives ~200 W m^{-2} of solar radiation during the year, and the bulk of that radiation is converted into heat at the surface, creating an average ground temperature 2.47 K warmer than the air temperature at 2 m. If the amount of locally absorbed radiation were to change over decades or centuries, such as through increased/decreased cloudiness, (de)forestation, or significant changes in the solar insolation, then we should expect $\Delta T_{\text{sgt-sat}}$ to change with time as well.

Recently, a great deal of work has been done on understanding the nature of the solar constant and its influence on the earth's climate system (Wild et al. 2005; Pinker et al. 2005). The sensitive dependence of $\Delta T_{\text{sgt-sat}}$ on the annual amount of incident solar radiation and the efficacy of a simple linear correction for the influence of solar radiation on ground temperatures provide us with a means to predict EPO's ground temperature response to temporal changes in the solar constant. Observations of mean surface incident solar radiation reported in Wild et al. (2005) suggest that various locations across the Northern Hemisphere have experienced increased radiation by as much as 5 W m^{-2} over the period 1992–2002. Our observations at EPO suggest that such a change in incident solar radiation could have led to as much as a 0.06 K trend in $\Delta T_{\text{sgt-sat}}$ during the past decade. Over longer periods of time, estimates of long-term changes in the solar constant are much more conservative. The Intergovernmental Panel on Climate Change (IPCC) estimates that over the period 1750–present, the change in solar forcing has been on the order of 0.3 W m^{-2} (Houghton et al. 2001), a value which would lead to a $\Delta T_{\text{sgt-sat}}$ offset at EPO of just 0.0036 K over the past century.

7. Conclusions

Ten years of detailed air and ground temperature monitoring at Emigrant Pass Observatory permit the following conclusions:

1) The surface ground temperature (z = 0) calculated from subsurface measurements at 0.1 m provides an accurate representation of the actual SGT at the site. This technique provides a better estimate of "skin" surface temperature than radiometry or embedding thermometers on or in the surface. SAT variations explain 94% of the variance in SGT ($z = 0$).
2) At EPO, the mean temperature difference $\Delta T_{\text{sgt-sat}}$ between the ground surface and the air sensor at 2 m averages 2.47 K from 1993 to 2004. Averaged over a diurnal cycle, this temperature difference falls between +14 and −10 K; over an annual cycle, $\Delta T_{\text{sgt-sat}}$ ranges from 2.3 to 2.5 K.
3) Incident solar radiation is the primary variable in determining the difference between ground and air temperatures ($\Delta T_{\text{sgt-sat}}$). This temperature difference increases 1.21 K for each 100 W m^{-2} of incident solar radiation. Therefore, $\Delta T_{\text{sgt-sat}}$ is often less than 1 K in the winter months when the solar radiation is less than 50 W m^{-2} and approaches 4 K during the summer months when the solar radiation can be as high as 350 W m^{-2}.
4) Much of the interannual variability in $\Delta T_{\text{sgt-sat}}$ at EPO is attributable to solar radiation changes. A linear update of $\Delta T_{\text{sgt-sat}}$ for variations in incident solar radiation is able to account for more than 90% of the interannual variability and suggests that the interannual variability is likely controlled by regional climate oscillations bringing more or less cloud cover to the area. Solar radiation can explain an additional 1.3% of the variance in SGT.
5) The influence of snow cover on $\Delta T_{\text{sgt-sat}}$ at EPO is primarily a seasonal increase in the amount of variability in $\Delta T_{\text{sgt-sat}}$ rather than a uniform bias of the mean annual ground–air temperature difference. Snow cover explains an additional 0.5% of the variance in SGT at EPO. The combined effects of SAT, incident solar radiation, and snow cover explain ~96% of the observed variance in SGT at the site.

This decade-long observational study of ground and air temperature tracking at EPO is a convincing demonstration that although ground and air temperatures are different, the two quantities track closely at annual and longer periods. This result provides strong support for the use of borehole temperature–depth profiles in climate change research. In particular, the high-fidelity tracking of SGT and SAT fully justifies the use of borehole-based climate reconstruction to estimate long-term changes in the SAT during and prior to the instrumental meteorological record. Additionally, this study also suggests that comparisons between borehole-based and proxy-based climate reconstructions calibrated on SAT observations are warranted.

Acknowledgments. This work was supported by the National Science Foundation under NSF Grants EAR-9706559 and EAR-0126029.

REFERENCES

Baker, D. G., and D. L. Ruschy, 1993: The recent warming in eastern Minnesota shown by ground temperatures. *Geophys. Res. Lett.,* **20,** 371–374.

Bartlett, M. G., D. S. Chapman, and R. N. Harris, 2004: Snow and the ground temperature record of climate change. *J. Geophys. Res.,* **109,** F04008, doi:10.1029/2004JF000224.

Beltrami, H., 2001: On the relationship between ground temperature histories and meteorological records: A report on the Pomquet station. *Global Planet. Change,* **29,** 327–348.

——, 2002: Climate from borehole data: Energy fluxes and temperatures since 1500. *Geophys. Res. Lett.,* **29,** 2111, doi:10.1029/2002GL015702.

Carslaw, H. S., and J. C. Jaeger, 1959: *Conduction of Heat in Solids*. 2d ed. Oxford University Press, 510 pp.

Chapman, D. S., and R. N. Harris, 1993: Repeat measurements in borehole GC-1, northwestern Utah: Towards isolating a climate-change signal in borehole temperature profiles. *Geophys. Res. Lett.,* **20,** 1891–1894.

——, D. Blackwell, W. Parry, W. Sill, S. Ward, and J. Whelan, 1978: Regional heat flow and geochemical studies in southwest Utah. Vol. 2, U.S. Geological Survey Rep. 14–08–0001–G–341.

Chisholm, T. J., and D. S. Chapman, 1992: Climate change inferred from analysis of borehole temperatures: An example from western Utah. *J. Geophys. Res.,* **97,** 14 155–14 176.

Delworth, T. L., and T. R. Knutson, 2000: Simulation of early 20th century global warming. *Science,* **287,** 2246–2250.

Geiger, R., 1965: *The Climate Near the Ground.* 4d ed. Harvard University Press, 611 pp.

Gonzalez-Rouco, F., H. von Storch, and E. Zorita, 2003: Deep soil temperature as proxy for surface air-temperature in a coupled model simulation of the last thousand years. *Geophys. Res. Lett.,* **30,** 2116, doi:10.1029/2003GL018264.

Harris, R. N., and D. S. Chapman, 1998: Geothermics and climate change 2: Joint analysis of borehole temperature and meteorological data. *J. Geophys. Res.,* **103,** 7371–7384.

——, and ——, 2001: Mid-latitude (30°–60°N) climatic warming inferred by combining borehole temperatures with surface air temperature. *Geophys. Res. Lett.,* **28,** 747–750.

Hu, Z., and S. Islam, 1995: Prediction of ground surface temperature and soil moisture content by the force-restored method. *Water Resour. Res.,* **31,** 2531–2539.

Huang, S., H. N. Pollack, and P. Y. Shen, 2000: Temperature trends over the past five centuries reconstructed from borehole temperatures. *Nature,* **403,** 756–758.

Irannejad, P., and Y. Shao, 1998: Description and validation of the Atmosphere–Land-Surface Interaction Scheme (ALSIS) with HAPEX and Cabauw data. *Global Planet. Change,* **19** (1–4), 87–114.

Jones, P. D., and A. Moberg, 2003: Hemispheric and large-scale surface air temperature variations: An extensive revision and an update to 2001. *J. Climate,* **16,** 206–223.

Karl, T. R., J. D. Tarpley, R. G. Quayle, H. F. Diaz, D. A. Robinson, and R. S. Bradley, 1989: The recent climate record: What it can and cannot tell us. *Rev. Geophys.,* **27,** 405–430.

Parton, W. J., 1984: Predicting soil temperatures in a shortgrass steppe. *Soil Sci.,* **138,** 93–101.

Peixoto, J. P., and A. H. Oort, 1992: *Physics of Climate.* AIP Press, 412 pp.

Pinker, R. T., B. Zhang, and E. G. Dutton, 2005: Do satellites detect trends in surface solar radiation? *Science,* **308,** 850–854.

Putnam, S. N., and D. S. Chapman, 1996: A geothermal climate-change observatory: First year results from Emigrant Pass Observatory in northwest Utah. *J. Geophys. Res.,* **101,** 21 877–21 890.

Ramaswamy, V., and Coauthors, 2001: Radiative forcing of climate change. *Climate Change 2001: The Scientific Basis,* J. T. Houghton et al., Eds, Cambridge University Press, 349–416.

Schmidt, W. L., W. D. Gosnold, and J. W. Enz, 2001: A decade of air-ground temperature exchange from Fargo, North Dakota. *Global Planet. Change,* **29,** 311–325.

Smerdon, J. E., H. N. Pollack, V. Cermak, J. W. Enz, M. Kresl, J. Safanda, and J. F. Wehmiller, 2004: Air-ground temperature coupling and subsurface propagation of annual temperature signals. *J. Geophys. Res.,* **109,** D21107, doi:10.1029/2004JD005056.

Soet, M., R. J. Ronda, J. N. M. Stricker, and A. J. Dolman, 2000: Land surface scheme conceptualization and parameter values for three sites with contrasting soils and climate. *Hydrol. Earth Syst. Sci.,* **4,** 283–294.

Tan, C. S., and R. C. Layne, 1993: Irrigation and ground cover management effect on soil temperature in a mature peach orchard. *Can. J. Plant Sci.,* **73,** 857–870.

Wild, M., and Coauthors, 2005: From dimming to brightening: Decadal changes in solar radiation at Earth's surface. *Science,* **308,** 847–850.